Third element effect in the surface zone of Fe-Cr-Al alloys

E. Airiskallio, E. Nurmi, M. H. Heinonen, I. J. Väyrynen, and K. Kokko*
Department of Physics and Astronomy, University of Turku, FI-20014 Turku, Finland and Turku University Centre for Materials and Surfaces (MatSurf), Turku, Finland

M. Ropo
Department of Information Technology, Åbo Akademi, FI-20500 Turku, Finland

M. P. J. Punkkinen
Department of Physics and Astronomy, University of Turku, FI-20014 Turku, Finland and Applied Materials Physics, Department of Materials Science and Engineering, Royal Institute of Technology, SE-10044 Stockholm, Sweden

H. Pitkänen and M. Alatalo
Department of Mathematics and Physics, Lappeenranta University of Technology, P.O. Box 20, FI-53851 Lappeenranta, Finland

J. Kollár
Research Institute for Solid State Physics and Optics, P.O. Box 49, Budapest H-1525, Hungary

B. Johansson
Applied Materials Physics, Department of Materials Science and Engineering, Royal Institute of Technology, SE-10044 Stockholm, Sweden and Department of Physics and Materials Science, Uppsala University, SE-75121 Uppsala, Sweden

L. Vitos
Applied Materials Physics, Department of Materials Science and Engineering, Royal Institute of Technology, SE-10044 Stockholm, Sweden; Research Institute for Solid State Physics and Optics, P.O. Box 49, Budapest H-1525, Hungary; and Department of Physics and Materials Science, Uppsala University, SE-75121 Uppsala, Sweden

(Received 26 October 2009; revised manuscript received 23 December 2009; published 27 January 2010)

The third element effect to improve the high temperature corrosion resistance of the low-Al Fe-Cr-Al alloys is suggested to involve a mechanism that boosts the recovering of the Al concentration to the required level in the Al-depleted zone beneath the oxide layer. We propose that the key factor in this mechanism is the coexistent Cr depletion that helps to maintain a sufficient Al content in the depleted zone. Several previous experiments related to our study support that conditions for such a mechanism to be functional prevail in real oxidation processes of Fe-Cr-Al alloys.

DOI: 10.1103/PhysRevB.81.033105 PACS number(s): 68.47.De, 68.35.Dv, 68.35.bd, 71.15.Nc

One of the best alloys regarding corrosion resistance at high temperature is Fe-Al. To maintain good oxidation resistance both the oxygen penetration through the oxide layer to the alloy and iron diffusion to the surface should be kept blocked. However, this blocking to be effective the Al concentration in bulk should be at least 10–15 at. %.[1] Unfortunately, this amount of Al makes the alloy very brittle consequently limiting the usability of Fe-Al in applications requiring ductile materials. However, the brittleness problem can be solved by adding, e.g., chromium to the alloy. Cr considerably improves the formation of the protective Al_2O_3 scale so that the amount of Al can be reduced to an acceptable level ensuring reasonable mechanical properties for the alloy.

Chromium addition to Fe-Al is an example of a more general so-called third element effect (TEE) frequently discussed in literature.[2] Adding 10 at. % Cr to Fe-Al, for instance, allows to reduce the Al concentration to 3 at. % without weakening the protecting layer at the surface.[2] Several phenomena have been proposed to be responsible for the observed TEE in Fe-Cr-Al alloys.[3] Early theories associated this effect to a transition from internal to external oxidation.[4] Later, it was argued that Cr can inhibit the external oxidation of Fe.[2] Most recently, Cr_2O_3 was considered as nucleation centers for the α-Al_2O_3, which may improve corrosion protection in contrast to the other transient aluminas.[5] At low temperatures Cr improves the oxidation resistance of Fe-Cr-Al due to the fast formation of Cr_2O_3 compared to that of α-Al_2O_3.[6,7] In this Brief Report, using a first-principles quantum-mechanical approach, we shed light on another possible mechanism responsible for the TEE in Fe-Cr-Al system. The proposed mechanism takes place under the surface through the interface between two different bulk regions. The first one is the deep bulk and the other one is the surface zone where the concentrations differ from those of the deep bulk due to, e.g., surface oxidation. However, it is worth to note that the proposed phenomenon is in principle quite general expected to appear in many ternary alloys whenever suitable conditions prevail.

Our computer modeling is based on the density-functional theory[8] in combination with the generalized gradient approximation.[9] The Kohn-Sham equations were solved using the exact muffin-tin orbitals (EMTO) method.[10–13] The EMTO method is based on the optimized overlapping

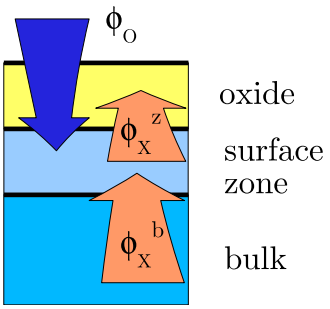

FIG. 1. (Color online) Schematic figure of the surface of an Fe-Cr-Al alloy. The surface zone tends to deplete from Al and Cr due to oxidation. ϕ_O and ϕ_X are the fluxes of oxygen and metal atoms, respectively. The superscripts b and z refer to the flux from deep bulk to the surface zone and from surface zone to the oxide scale, respectively.

muffin-tin approximations. Within this approximation, the spherical muffin-tin wells and the constant potential from the interstitial are derived self-consistently by solving the integro-differential equations obtained from the condition that the difference between the corresponding full-potential and the muffin-tin model potential to be minimum. Further details about the optimization technique can be found in Ref. 14. Since the present investigation maps large concentration intervals, with Cr and Al concentrations approaching zero, the conventional supercell method would require enormously large supercells. Here, we resolved this difficulty by employing the coherent potential approximation (CPA) (Ref. 15) as implemented within the frameworks of the EMTO method.[13,16] The EMTO-CPA approach has been applied successfully in the theoretical study of various structural and electronic properties of Fe-based alloys demonstrating the accuracy and efficiency needed for the present investigation.[13] Calculations were carried out for Fe-Cr-Al alloys containing up to 20 at. % Cr and 10 at. % Al. These alloys were modeled as substitutional disordered ferromagnetic body-centered-cubic (bcc) alloys. For each system the theoretical equilibrium lattice constant was used. The effective chemical potential $(\mu_{Fe}-\mu_{Al})$, describing the Al→Fe exchange process, was calculated from the first-order derivative of the total energy with respect to Al content by keeping the volume and the Cr concentration constant.[17,18]

High oxygen affinity of Al (Ref. 19) assists the Al depletion of the surface zone (Fig. 1) of an Fe-Al alloy during the surface oxidation.[2,20] The formation of the depleted zone is considered to be one of the main causes for the breakdown of the oxidation resistance of Fe-Al alloys.[1] The most straightforward way to prevent this destructive Al-depleted surface zone from growing up is to increase the Al content in the bulk. However, considering $(\mu_{Fe}-\mu_{Al})$ with different compositions (Fig. 2) suggests an alternative mechanism to preserve the necessary Al level in the surface zone. The key factor in this mechanism turns out to be the coexistent Cr depletion. To elucidate this we expand on the atomic processes between the deep bulk and the surface zone that can possibly affect the oxide formation on the alloy surface. First, we propose a mechanism for Al enrichment in the surface zone and then discuss some possible effects of this

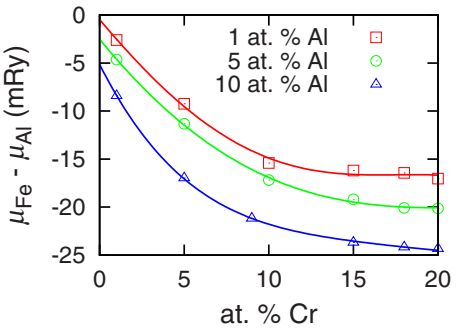

FIG. 2. (Color online) The calculated chemical potential difference $\mu_{Fe}-\mu_{Al}$ for Fe-Cr-Al as a function of Cr and Al content. The curves are polynomial fits to the calculated data points shown in the figure. The zero level corresponds to –2059.919 Ry.

mechanism with comparison to experimental observations.

According to Fig. 2, in the surface zone the depletion of both Al and Cr increases the Fe chemical potential with respect to that of Al. The induced imbalance of the chemical potentials in the alloy may lead to the Al↔Fe exchange processes between the deep bulk and the surface zone. This apparently has important consequences on the chemical composition in the surface zone (Fig. 1). Namely, a Cr depletion in the surface zone will increase the probability of Al to diffuse from bulk to the depletion zone and thus tending to restore the relative Al concentration beneath the oxide layer. To make the suggested mechanism more clear, we sketch in Fig. 3 one possible sequence of atomic processes beginning at a stage when the surface zone has not yet depleted; i.e., the considered alloy is homogeneous from bulk to the surface. The initial state of the surface zone (and bulk) is represented as a circle of orange color. If Al depletion is accompanied with Cr depletion (red arrow upward) the chemical potential of Fe relative to that of Al in the surface zone is further increased compared to the case when there would be only the depletion of Al. In Fig. 3, the depleted state of the surface zone is represented by the head of the arrow pointing up and

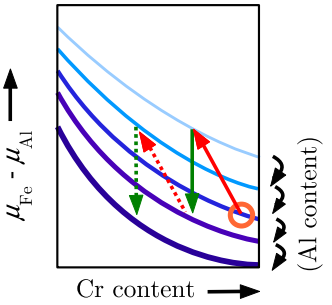

FIG. 3. (Color online) Schematic plot of $\mu_{Fe}-\mu_{Al}$ as a function of Cr content with Al content as a parameter. The Al content increases from curve to curve downward. By the sequence of the arrows we illustrate both the changes in the concentrations and $\mu_{Fe}-\mu_{Al}$ within the surface zone during the Al and Cr depletion and the subsequent Al recovering of the surface zone (SZ). $\mu_{Fe}-\mu_{Al}$ in three different stages are: 1) initially in the SZ: orange circle; 2) Al- and Cr-depleted SZ: head of the red arrow (upward); 3) Al recovered SZ: head of the green arrow (downward). Second process in cascade: the dashed arrows.

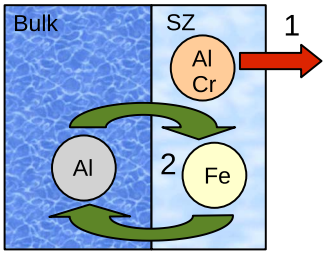

FIG. 4. (Color online) If SZ is depleted with Al and Cr, process 1 (upward arrow in Fig. 3), the driving force for Fe↔Al exchange between deep bulk and SZ increases, process 2 (downward arrow in Fig. 3).

leftward. Since the integrated interdiffusion constant of Cr is much lower than that of Al and Fe,[21] it is expected that Cr diffusion plays a minor role in the subsequent recovering process and therefore the arrow representing the healing of the depleted zone is pointing downward. The combined process is not reversible tending to bring the surface zone enriched with Al compared to the bulk alloy. Besides the chemical potentials viewpoint (Fig. 3) the atomic perspective (Fig. 4) on the above processes is also helpful in taking the general view of the combined process. When the surface is in a state that the protective scale has not fully formed, or it has been broken, Cr-rich oxide formation occurs leading to the formation of Cr-depleted regions. Depending on the external conditions, temperature, state of the oxidation, etc., a certain steady-state situation of the surface zone will be reached (end point of the sequence of the arrows in Fig. 3). However, as long as the Cr concentration in the surface zone is less than its average bulk value the replacement of the depleted Al in the surface zone is more efficient than in Fe-Al alloys. We note that one straightforward consequence of the above Cr-driven Al-pump phenomenon is that in Fe-Cr-Al alloys the Cr and Al concentrations as well as their gradients should show a clear anticorrelation.

To find out whether in real systems the prerequisites for the suggested Al enrichment process in the surface zone are realized we consider the data obtained in surface oxidation experiments of Fe-Cr-Al with bulk composition of ~20 at. % Cr and ~5 at. % Al.[22] The measured atomic fractions suggest that the native oxide layer formed at ambient atmosphere ($x_{Al} \approx 0.10$, $x_{Cr} \approx 0.12$, $x_{Fe} \approx 0.31$, and $x_O \approx 0.47$, i.e., relative to the total number of metal atoms Cr has increased to ~23 at. % and Al to ~19 at. %) is enriched in Al and Cr implying Al- and Cr-depleted alloy phases below the oxide scale. The integrated relative concentration of the alloy component i in the oxide layer at oxidation time t is

$$x_i(t) = \frac{\int_0^t \phi_i d\tau}{\int_0^t \Phi d\tau},$$

where ϕ_i and Φ are the flux of the component i and the total flux from the alloy phase to the oxide phase. From the above expression we obtain $\mathrm{sgn}(dx_i/dt) = \mathrm{sgn}[\phi_i/\Phi - x_i(t)]$, i.e., increasing concentration corresponds to increasing relative flux (ϕ_i/Φ) compared to the average flux $(\langle\phi_i\rangle/\langle\Phi\rangle)$ and vice versa. During the first minute oxidation at 670 °C, the experimental slopes of the relative concentrations show the following trends:[22]

$$\frac{dx_{Al}}{dt} \approx 0, \quad \frac{dx_{Cr}}{dt} > 0, \quad \frac{dx_{Fe}}{dt} < 0, \quad \left|\frac{dx_{Cr}}{dt}\right| < \left|\frac{dx_{Fe}}{dt}\right|.$$

Therefore, the trends of the initial relative fluxes of Al, Cr, and Fe have approximately constant, slightly increasing and decreasing behaviors, respectively. At about 1 min oxidation time the experimental slopes of the relative atomic concentrations change to[22]

$$\frac{dx_{Al}}{dt} > 0, \quad \frac{dx_{Cr}}{dt} \approx \frac{dx_{Fe}}{dt} < 0, \quad \left|\frac{dx_{Fe}}{dt}\right| < \left|\frac{dx_{Al}}{dt}\right|$$

implying reducing relative fluxes for Cr and Fe and increasing relative flux for Al.

Interpreting the above experimental data in terms of relative fluxes describing the transformation from the base metal to the metal oxide the following scenario can be constructed. The observed relative Al enrichment (about four times compared to the average bulk alloy value) in the measurement of the oxide scale formed during the initial ambient oxidation can be attributed to the high oxygen affinity of Al and the Al enriched surfaces of the base alloy at equilibrium as a result of the lower surface energy of Al compared to that of Cr and Fe.[24,25] During the first minute oxidation, the Cr concentration reaches its maximum in the oxide layer which means that the Cr depletion in the alloy phase also reaches its peak. After 1 min oxidation, the relative flux of Al takes over the relative fluxes of Cr and Fe. The increasing Al flux can be associated with the increased Al concentration in the Cr-depleted surface zone just below the oxide layer.

A large number of experiments support the suggested Cr-driven Al pump to be operative in the enhancement of the oxidation resistance of Fe-Cr-Al alloys. There exists also direct observations of the depletion of Al and Cr in Fe-Cr-Al.[23] The phase separation investigations for Fe-Cr-based alloys show that Al preferentially partitions in the Fe-rich α phase rather than in the Cr-rich α' phase.[26–29] The anticorrelation between the Cr and Al concentrations is observed also within the oxide layer formed on the surface of an Fe-Cr-Al alloy.[5] The oxide scale grows both outward and inward compared to the position of the initial unoxidized surface. The measured inward gradient of the Cr concentration is negative whereas that of Al is positive suggesting the Cr depletion and Al accumulation in the vicinity of the oxide layer.

There are both direct and indirect experimental evidence of Cr depletion in Fe-Cr-Al. Here we list a few of them. Corrosion resistance experiments for Fe-Cr-Al alloys show Cr depletion in the Fe-10Al-5Cr alloy.[30] In the oxidation experiments of Fe_3Al-(0,2,4,6%)Cr alloys a Cr-free region was observed.[31] In low Al or Si iron-chromium alloys the inward growth of Cr_2O_3 was deduced to be initiated due to

the Cr-depleted zone.[32] The depletion of Cr is observed also in ferritic steels.[33] Oxidizing experiments on aluminized $Fe_{0.7}Cr_{0.3}$ at various temperatures[34] also show traces of Al pump. The changes in Cr and Al concentrations and gradients are always found to have opposite trends. We conclude that the key parameter for the observed anticorrelation between the Cr and Al concentrations in oxidized Fe-Cr-Al alloys is the Cr concentration since the Cr depletion under the oxide layer is also observed in Fe-Cr binary alloys.[35] The proposed TEE mechanism has its origin in the effect of the third element on the mixing enthalpy (ΔH) of bcc Fe-Al and Fe-Cr alloys.[36] The decreasing $(\mu_{Fe}-\mu_{Al})$ with Al and Cr addition is simply the consequence of $\partial \Delta H/\partial c_{Al}$ being an increasing function with respect to both Al and Cr concentrations.

The computer resources of the Finnish IT Center for Science (CSC) and Mgrid project are acknowledged. Financial support from the Academy of Finland (Grant No. 116317) and Outokumpu Foundation are acknowledged. Part of this work was supported by the Swedish Research Council, the Carl Tryggers Foundation, and the Hungarian Scientific Research Fund (Grant No. T048827). E.N. is indebted to National Graduate School in Materials Physics for partial funding.

*kalevi.kokko@utu.fi

[1] P. Tomaszewicz and G. R. Wallwork, High. Temp. Sci. **4**, 75 (1978).
[2] Y. Niu, S. Wang, F. Gao, Z. G. Zhang, and F. Gesmundo, Corros. Sci. **50**, 345 (2008).
[3] F. H. Stott, G. C. Wood, and J. Stringer, Oxid. Met. **44**, 113 (1995).
[4] C. Wagner, Corros. Sci. **5**, 751 (1965).
[5] H. Götlind, F. Liu, J.-E. Svensson, M. Halvarsson, and L.-G. Johansson, Oxid. Met. **67**, 251 (2007).
[6] H. Josefsson, F. Liu, J.-E. Svensson, M. Halvarsson, and L. G. Johansson, Mater. Corros. **56**, 801 (2005).
[7] G. Berthomé, E. N'Dah, Y. Wouters, and A. Galerie, Mater. Corros. **56**, 389 (2005).
[8] P. Hohenberg and W. Kohn, Phys. Rev. **136**, B864 (1964).
[9] J. P. Perdew, K. Burke, and M. Ernzerhof, Phys. Rev. Lett. **77**, 3865 (1996).
[10] O. K. Andersen, O. Jepsen, and G. Krier, in *Lectures on Methods of Electronic Structure Calculations*, edited by V. Kumar, O. K. Andersen, and A. Mookerjee (World Scientific Publishing Co., Singapore, 1994), p. 63.
[11] L. Vitos, H. L. Skriver, B. Johansson, and J. Kollár, Comput. Mater. Sci. **18**, 24 (2000).
[12] L. Vitos, Phys. Rev. B **64**, 014107 (2001).
[13] L. Vitos, *Computational Quantum Mechanics for Materials Engineers: The EMTO Method and Applications*, Engineering Materials and Processes Series (Springer-Verlag, London, 2007).
[14] M. Zwierzycki and O. K. Andersen, Acta Phys. Pol. A **115**, 64 (2009).
[15] P. Soven, Phys. Rev. **156**, 809 (1967); B. L. Györffy, Phys. Rev. B **5**, 2382 (1972).
[16] L. Vitos, I. A. Abrikosov, and B. Johansson, Phys. Rev. Lett. **87**, 156401 (2001).
[17] The basis set included *s*, *p*, *d*, and *f* orbitals. The one-electron equations were solved within the scalar-relativistic and soft-core approximation. The Green's function was calculated for 16 complex energy points distributed exponentially on a semicircular contour including states within 1 Ry below the Fermi level. In the one-center expansion of the full charge density, we adopted an *l* cutoff of 8 and the total energy was calculated using the full charge density technique (Refs. 12 and 13). From a convergence test of the total energy with respect to the number of **k** vectors we found that 506 uniformly distributed **k** vectors in the irreducible wedge of the bcc Brillouin zone was enough for present purposes.
[18] M. Ropo, K. Kokko, L. Vitos, J. Kollár, and B. Johansson, Surf. Sci. **600**, 904 (2006).
[19] J. Camra, E. Bielańska, A. Bernasik, K. Kowalski, M. Zimowska, A. Białas, and M. Najbar, Catal. Today **105**, 629 (2005).
[20] Z. G. Zhang, F. Gesmundo, P. Y. Hou, and Y. Niu, Corros. Sci. **48**, 741 (2006).
[21] P. C. Tortorici and M. A. Dayananda, Mater. Sci. Eng., A **244**, 207 (1998).
[22] P. Hou, J. Am. Ceram. Soc. **86**, 660 (2003).
[23] I. G. Wright, R. Peraldi, and P. A. Pint, Mater. Sci. Forum **461-464**, 579 (2004).
[24] M. Aldén, H. L. Skriver, S. Mirbt, and B. Johansson, Surf. Sci. **315**, 157 (1994).
[25] L. Vitos, A. V. Ruban, H. L. Skriver, and J. Kollár, Surf. Sci. **411**, 186 (1998).
[26] C. Capdevila, M. K. Miller, and K. F. Russell, J. Mater. Sci. **43**, 3889 (2008).
[27] C. Capdevila, M. K. Miller, K. F. Russell, J. Chao, and J. L. Conzález-Carrasco, Mater. Sci. Eng., A **490**, 277 (2008).
[28] H. G. Read, H. Murakami, and K. Hono, Scr. Mater. **36**, 355 (1997).
[29] F. Zhu, H. Wendt, and P. Haasen, Scr. Metall. **16**, 1175 (1982).
[30] R. M. Deacon, J. N. DuPont, C. J. Kiely, A. R. Marder, and P. F. Tortorelli, Oxid. Met. **72**, 87 (2009).
[31] D. B. Lee, G. Y. Kim, and J. G. Kim, Mater. Sci. Eng., A **339**, 109 (2003).
[32] F. H. Stott and F. I. Wei, Oxid. Met. **31**, 369 (1989).
[33] P. Huczkowski, N. Christiansen, V. Shemet, J. Piron-Abellan, L. Singheiser, and W. J. Quadakkers, Mater. Corros. **55**, 825 (2004).
[34] C. Houngniou, S. Chevalier, and J. P. Larpin, Oxid. Met. **65**, 409 (2006).
[35] M. E. Somervuori, L.-S. Johansson, M. H. Heinonen, D. H. D. van Hoecke, N. Akdut, and H. E. Hänninen, Mater. Corros. **55**, 421 (2004).
[36] M. Ropo, K. Kokko, M. P. J. Punkkinen, S. Hogmark, J. Kollár, B. Johansson, and L. Vitos, Phys. Rev. B **76**, 220401(R) (2007).